J. Great Lakes Res. 13(4):515-529
Internat. Assoc. Great Lakes Res., 1987

LAGRANGIAN COMPARISON OF OBJECTIVELY ANALYZED AND DYNAMICALLY MODELED CIRCULATION PATTERNS IN LAKE ERIE

David J. Schwab and John R. Bennett
Great Lakes Environmental Research Laboratory
National Oceanic and Atmospheric Administration
Ann Arbor, Michigan 48105

ABSTRACT. Currents measured at 28 moorings in Lake Erie during May through October, 1979, were low-pass filtered to remove energy at diurnal, inertial, and higher frequencies. The current meter observations were interpolated to a regular grid over the lake by a new objective analysis technique, producing a streamfunction field which 1) conserves mass both locally and globally, 2) has values on the shores given by known river flows, 3) has the correct currents where they were measured, and 4) minimizes a function of squared vorticity in areas between the observations. In addition, a numerical, time-dependent, barotropic, rigid-lid circulation model was run using winds from six meteorological buoys on the lake as the forcing function. Twelve 5-day storm cases were selected for detailed Lagrangian analysis. At the beginning of each case, marker particles were released into the objectively analyzed and dynamically modeled flow fields at each of the 28 current meter mooring locations. Differences in the particle trajectories were analyzed by location and as a function of time. The results indicate that the circulation model shows some skill in generating particle trajectories over the course of a storm event in the central basin of the lake with mean positional differences as low as 8.5 km after 5 days compared to a mean path length of 14.9 km. They also show how numerical models and the objective analysis technique can be used to design more effective instrument deployment schemes for measuring lake and ocean circulation patterns.
INDEX WORDS: Water circulation, mathematical models, water currents.

INTRODUCTION

The subject of this paper is the comparison of low-frequency (sub diurnal and inertial) fluctuations in currents observed in Lake Erie with numerical model predictions. Several previous studies have examined the same subject in Lake Erie and other lakes (see Simons 1980 for a summary), but most of them have tried to verify the numerical models by comparing observed currents from individual moorings to currents calculated by the numerical models at the same point. The inherent problem in this approach is that although the model may be reproducing the large-scale features of the actual current field, point-by-point comparisons of calculated and observed currents may still show significant differences. An alternative approach is to concentrate instrumentation along a transect so that accurate mass transport comparisons can be made between model results and observations. Simons (1985) used this method in Lake Ontario to further explore the question of why the linear numerical models seem to provide accurate simulations of the lake's circulation for time scales on the order of 3-10 days, but seem to fail for seasonal or annual time scales. We would like to propose yet another approach for verifying circulation models in cases where the field observations provide adequate spatial resolution to infer lake-wide circulation patterns. This approach is to use the available observations to determine an "observed" lake scale circulation pattern using a two-dimensional objective analysis technique and then compare the observed circulation pattern to the computed circulation pattern in terms of particle trajectories. Using particle trajectories has two advantages compared to point-to point comparisons of current time series of mass balance across a transect. First, the differences between observed and computed circulation patterns can be more easily visualized.

Second, it emphasizes the long-term drift instead of the small time and space scale fluctuations which are poorly sampled by current meters. We could also have compared time series of observed and modeled current vectors in terms of progressive vector diagrams to achieve similar results, but we felt that by comparing particle trajectories a more useful error statistic (distance between particles moved by computed and observed currents) would be generated. In the real lake, as pointed out by a reviewer, particle trajectories are not uniquely defined due to turbulence and diffusion. That is, two particles released at nearly the same location do not necessarily follow nearly the same path. However, in the numerical realization of the objectively analyzed currents, particle trajectories are uniquely determined because all random effects have been filtered out. Therefore, the trajectories produced by objective analysis and numerical model currents are deterministic and not stochastic processes.

Current observations in the Great Lakes or in coastal regions of the ocean are strongly influenced by the presence of boundaries. The boundaries constrain the flow to be more parallel to the shore as it gets closer to the shore, causing large variations in the ratio of cross-isobath to along-isobath variance in the currents (see, for example, Murthy and Dunbar 1981). This fact makes it difficult to apply the type of objective analysis techniques used in the MODE experiment (Freeland and Gould 1976) or in other deep open ocean experiments like Saunders (1983). Galt (1980) suggested a method for inferring circulation patterns in coastal regions from a limited amount of current observations, but his technique is more akin to fitting dynamical model results to observed data by adjustment of the free parameters. Lam (1981) proposed a method for objective analysis of currents in closed or open regions which minimizes the variance of the difference between a crude guess at the interpolated (observed) current field and the final field subject to the constraint that the final field satisfies the continuity equation. Unfortunately, the results of this type of technique depend strongly on the initial guess for the current field, particularly in data sparse regions. Rao and Schwab (1981) used a set of orthogonal streamfunction modes determined by the topography of a closed basin as the basis for an expansion of the interpolated current field. By fitting the expansion to the observed currents at observation points, the expansion coefficients are uniquely determined. However, the number of basis functions included in the expansion is limited by the number of current observations available and the choice of which functions to include in the expansion is somewhat arbitrary. The objective analysis technique introduced in this paper attempts to remedy some of these problems.

DATA

The data consist of current observations from 56 current meters deployed on 28 moorings in Lake Erie by the Great Lakes Environmental Research Laboratory (GLERL) and the National Water Research Institute (NWRI) of Canada during the months of May-October, 1979. Figure 1 shows the locations of the moorings and partitions the lake into four sections based on the density of the current meter array in each area. Area 1, the western basin, contains only three moorings. Area 2, the central basin, has the best spatial coverage with 14 moorings. Area 3, the ridge, has fair coverage with six moorings and Area 4, the eastern basin, has only a single transect consisting of five moorings. Most moorings consisted of two vector-averaging current meters, one 10 m below the surface and the other 3 m off the bottom. Some of the shallower moorings had only one meter and some of the deeper moorings had meters at intermediate depths. The most significant factor about the measurement program for the purpose of this paper was that the spatial coverage of the moorings, at least in the central basin of the lake (Area 2), was sufficiently dense to be useful for inferring a lake-scale circulation pattern.

The raw current meter data were digitally filtered to remove energy at frequencies higher than 0.75 cycles per day. This effectively removed diurnal, inertial, and gravitational oscillations from the records. The data were then sampled at 6-h intervals to provide time series for further analysis. The 6-h interval was chosen to provide sufficient time resolution for accurate trajectory calculations (at least 4 points during the shortest fluctuation period).

In addition to the current measurements, NWRI operated six meteorological buoys in the lake during the field program. Their locations are shown by the open circles in Figure 1 (three of the meteorological buoys were co-located with current meter moorings 10, 13, and 27). The buoys measured wind speed, wind direction, and air tempera-

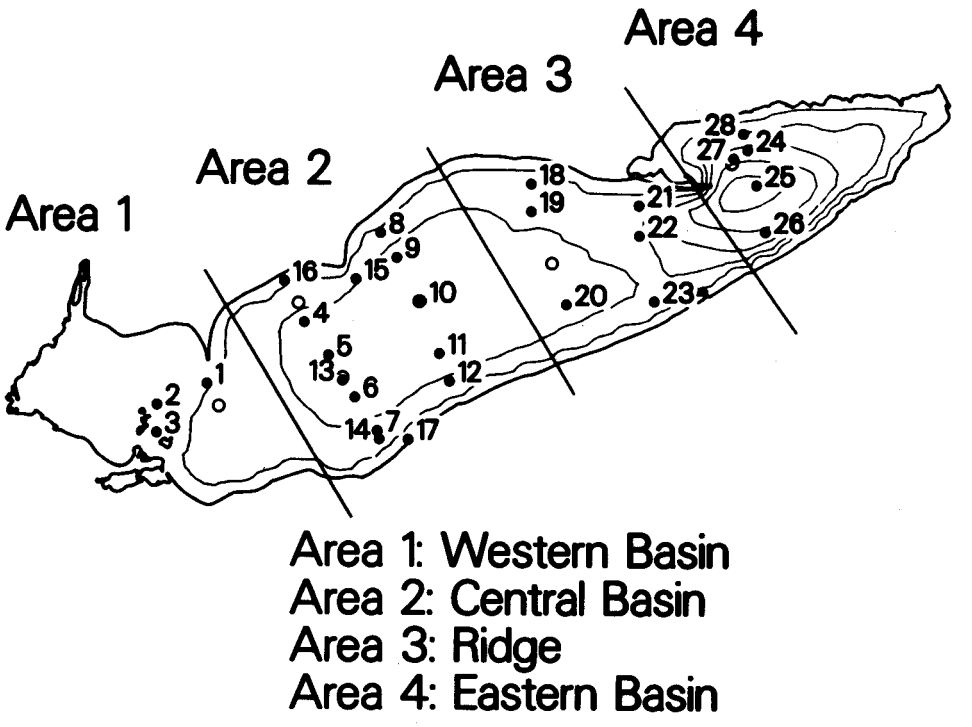

FIG. 1. Location map for Lake Erie 1979 moorings. Filled circles are current meter moorings, open circles are meteorological buoy moorings. Depth contours are at 10-m intervals.

ture at 4 m above the water surface, and surface water temperature. From these data we assembled a time series of surface wind stress fields using the methods described in the next section.

Figure 2 shows time series of spatially averaged longitudinal and transverse wind stress in addition to the mean squared current speed from all the moorings for the entire observation period, May–October. It is immediately evident that the energy of the currents in the lake rises above a relatively low background level of 20–50 $cm^2\ sec^{-2}$ only during a few brief episodes that are highly correlated to peaks in the wind stress input. We therefore selected 12 5-day cases, that together account for almost half of the energy input to the lake, for detailed comparison of trajectory calculations from objectively analyzed and numerically modeled currents. During periods outside the high energy cases, particle motions are too small to make meaningful comparisons. The 12 cases chosen are shown by the horizontal bars in Figure 2.

METHODS

Objective Analysis Method

An objective analysis method was developed to interpolate the observed currents to a rectangular grid system covering the entire lake. The method provides a current field that 1) conserves mass both locally and globally, 2) has values on the shores given by known river flows, 3) has the correct currents where they were measured, and 4) minimizes a function of squared vorticity in areas between the observations. The flow field is assumed to be nondivergent so that the eastward and northward components of the vertically-averaged flow (u, v) can be represented by a streamfunction, ψ, as

$$u = -\frac{1}{h}\frac{\partial \psi}{\partial y} \tag{1}$$

$$v = \frac{1}{h}\frac{\partial \psi}{\partial x} \tag{2}$$

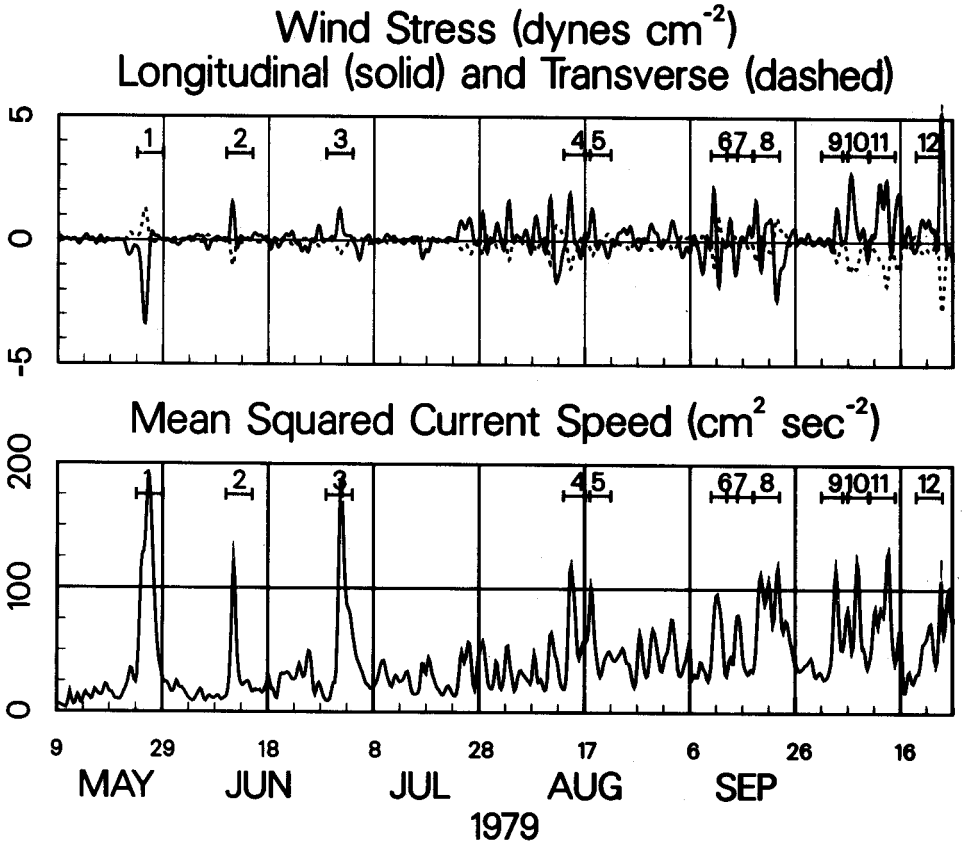

FIG. 2. Average longitudinal and transverse wind stress components (dynes cm^{-2}) and mean squared current speed during May - October 1979 in Lake Erie. Horizontal bars numbered 1 - 12 indicate 12 cases selected for consideration in this paper.

where h is depth. The objective analysis technique consists of applying the finite difference analogues of (1) and (2) at all current measurement points using a discretized streamfunction (values of streamfunction are only defined at the corners of the rectangular grid boxes covering the lake). Let n represent the number of measurement points and m represent the number of streamfunction points on the finite-difference grid. Then the above procedure results in a system of 2n linear equations involving some of the m unknown streamfunction values. Generally the number of streamfunction points is much larger than the number of measurement points so that the system is underdetermined. Another condition is required to solve the system.

There are several options possible for constraints to determine a unique solution. Saunders (1983) chose to require that the gridpoints between the current meters have the same statistics as the known points. For many of our intended applications (trajectory forecasting, for example) we would rather interpolate a smooth solution or weak currents where observational information is sparse. With a prediction of zero current, the error can be no larger than the actual current, where other interpolation methods can give unknown errors. A natural way to create a smooth solution is to require the square of the Laplacian to be as small as possible. If the finite difference version of

$$\nabla^2\psi = 0 \qquad (3)$$

is applied at each grid point, the system of algebraic equations for the unknown stream function values is overdetermined instead of underdetermined. A least squares solution of the system can then be computed under the condition that the equations generated by the current observations are given a higher weight than the smoothness con-

straints. One of the properties of this Laplacian smoothing is that far from the observations, the currents decay to zero.

The Laplacian of the stream function is proportional to the vorticity of the flow in a flat basin. In a variable depth basin the vorticity is

$$\eta = \frac{\partial v}{\partial x} - \frac{\partial u}{\partial y} = \nabla \cdot h^{-1} \nabla \psi. \quad (4)$$

We experimented with several constraints of the form $h^{\alpha}\eta$, testing them against currents computed from the numerical solution used in Bennett and Campbell (1986) for wind-driven circulation in a circular basin. The best results were obtained for a value of the exponent approximately equal to 1. Using this value, the error monotonically decreased as the number of current observations increased and the kinetic energy was well-behaved, only slightly exceeding the exact value in some cases. Thus, the function minimized is the depth-weighted squared vorticity,

$$E = (h\nabla \cdot h^{-1} \nabla \psi)^2 = \text{minimum} \quad (5)$$

It is possible that other functions such as $\nabla^2\psi$, which eliminates the depth dependence, could also be used, but we chose (4).

The finite difference form of Eq. 5 provides a linear equation for the unknown stream function values at each of the m interior stream function points. When a value for ψ on the boundary is required, either $\psi = 0$ is specified or appropriate values for any river inflows and outflows are used. Together with the 2n equations provided by Eqs. 1 and 2 for the n current meter observations, the system consists of $2n + m$ equations in m unknowns and can be solved in a least squares sense by standard procedures. The weight given to the streamfunction equations was 0.0001 times the weight given to the current meter equations (after Δs is used to give them the same units). This value is small enough that, for all practical purposes, the current meter equations are satisfied exactly.

The objective analysis procedure was applied to low-pass filtered current meter observations from the 28 moorings shown in Figure 1 for each of the 12 5-day cases. A stream function field was produced at intervals of 6 hours during each case. A 10-km grid covering the lake was used and the Detroit River inflow and Niagra River outflow were fixed at 5,700 $m^3 s^{-1}$.

Circulation Model

The numerical circulation model is the same barotropic rigid-lid model used by Schwab (1983). The model is based on the linearized vorticity equation

$$\frac{\partial}{\partial t}(\nabla \cdot h^{-1} \nabla \psi) + J(\psi, h^{-1} f) = \vec{k} \cdot \text{curl} \left(\frac{\vec{\tau}_s - \vec{\tau}_b}{\rho h} \right) \quad (6)$$

where f is the Coriolis parameter, $\vec{\tau}_s$ is surface stress, $\vec{\tau}_b$ is bottom stress, $\vec{k}$ is a vertical unit vector, and J is the Jacobian operator. Eq. (6) is discretized and solved at each time step by a relaxation scheme (Schwab *et al.* 1981). The bottom stress is defined as

$$\frac{\vec{\tau}_b}{\rho} = C_D |\vec{v}| \vec{v} \quad (7)$$

where $\vec{v}$ is the velocity vector from the current timestep and $|\vec{v}|$ is calculated from the previous timestep. The drag coefficient, C_D, was initially assigned a value of 0.002 based on the experience of other circulation modeling efforts with this type of bottom friction formulation. However, after initial comparison of average computed current speeds to average observed speeds, the drag coefficient was increased to a value of 0.008 providing closer agreement between computed and observed current speeds. Note that in (7), $\vec{v}$ should actually be the bottom velocity, not the vertical mean. If the bottom velocity is less than the vertical mean, a lower drag coefficient would be necessary when using vertical mean currents in (7). It may be that the currents in the thin hypolimnion that persists in the central basin for much of the summer are actually higher than the vertical mean currents. The model was run on a 5-km grid covering Lake Erie with a 1-hour time step for the entire May-October period and currents were saved at 6-hour intervals.

The wind stress field in the numerical model is based on observations at the six meteorological buoys. Wind speed and direction are converted to vector wind stress at each station using an aerodynamic drag coefficient based on the Businger *et al.* (1971) formulation for stability length and Charnock's (1955) formula. This procedure produces a drag coefficient which increases with wind speed, increases when the air temperature is less than the water temperature, decreases when the air

temperature is greater than the water temperature, and has a value of 1.62×10^{-3} for neutral conditions with a wind speed of 15 m s^{-1} at 10-m height (Schwab 1978). Spatial interpolation is accomplished by expressing the two wind stress components as linear functions of the spatial coordinates, i.e.,

$$\frac{\tau_s^x}{\rho} = ax + by + c \tag{8}$$

$$\frac{\tau_s^y}{\rho} = dx + ey + f \tag{9}$$

The coefficients (a-f) are determined by least-squared fitting to the stress components at the observation points. Although Lake Erie is stratified during the May-October period, we feel we are justified in using a barotropic model for this comparison. Simons (1976) found that the results from a one-layer and a two-layer numerical model of Lake Erie showed a difference in current magnitude in the central basin (the two-layer model currents were higher), but, in general, that the character of the two-layer solution was similar to the one-layer solution except in the southwestern corner of the central basin. Schwab's (1983) results for circulation patterns in Lake Michigan showed good correlation between barotropic model results and observed current fluctuations in the 3–10 day period range during April-November, 1976. We feel that the barotropic model will be able to simulate the storm-induced circulation patterns in Lake Erie, even during the stratified period.

Particle Trajectories

Once the currents from an objective analysis scheme or a numerical model are available on a rectangular grid covering the lake, it is a relatively straightforward procedure to compute particle trajectories. The equations governing current-induced particle motion are

$$\frac{dx}{dt} = u(x,y) \tag{10}$$

$$\frac{dy}{dt} = v(x,y) \tag{11}$$

where x and y are the particle displacements along Cartesian axes from a specified origin. As shown by Bennett and Clites (1987), some care must be taken in the numerical integration of Eqs. (10) and (11) to ensure that particles do not artificially slow down near jagged boundaries or get trapped in the corners of the finite difference grid. In the numerical scheme, the u and v components of the current are interpolated to the corners of each grid box in a way that prevents the production of artificial "dead" zones in corner grid boxes and guarantees that the currents will never move a particle across a shoreline boundary. Then a second-order finite difference scheme is used to numerically integrate (10) and (11). The scheme is given by

$$\frac{x^{n+1} - x^n}{\Delta t} = u(x^n,y^n) + \frac{1}{2}\frac{\partial u}{\partial x}(x^{n+1} - x^n) + \frac{1}{2}\frac{\partial u}{\partial y}(y^{n+1} - y^n) \tag{12}$$

and

$$\frac{y^{n+1} - y^n}{\Delta t} = v(x^n,y^n) + \frac{1}{2}\frac{\partial v}{\partial x}(x^{n+1} - x^n) + \frac{1}{2}\frac{\partial v}{\partial y}(y^{n+1} - y^n) \tag{13}$$

The values of u, v, and their derivatives are computed by bilinear interpolation in each grid box from the values of u and v at the four corner points of the grid square in which the particle begins the time step. The time step is adjusted dynamically to ensure that the fastest currents don't move a particle farther than 1/8 of a grid interval in a single time step.

Bennett and Clites (1987) tested this scheme with a solid rotation circulation pattern in a circular basin and found that a grid interval of about 1/20 the radius of the basin was required for accurate simulation of a complete circuit of the basin by a particle near the shore.

A single particle was released at each current meter mooring shown in Figure 1 at the beginning of each 5-day case. Particle trajectories were then calculated based on currents from the objective analysis procedure and currents from the numerical circulation model. Particle locations 1-, 2-, 3-, 4-, and 5-day intervals after release were recorded and compared.

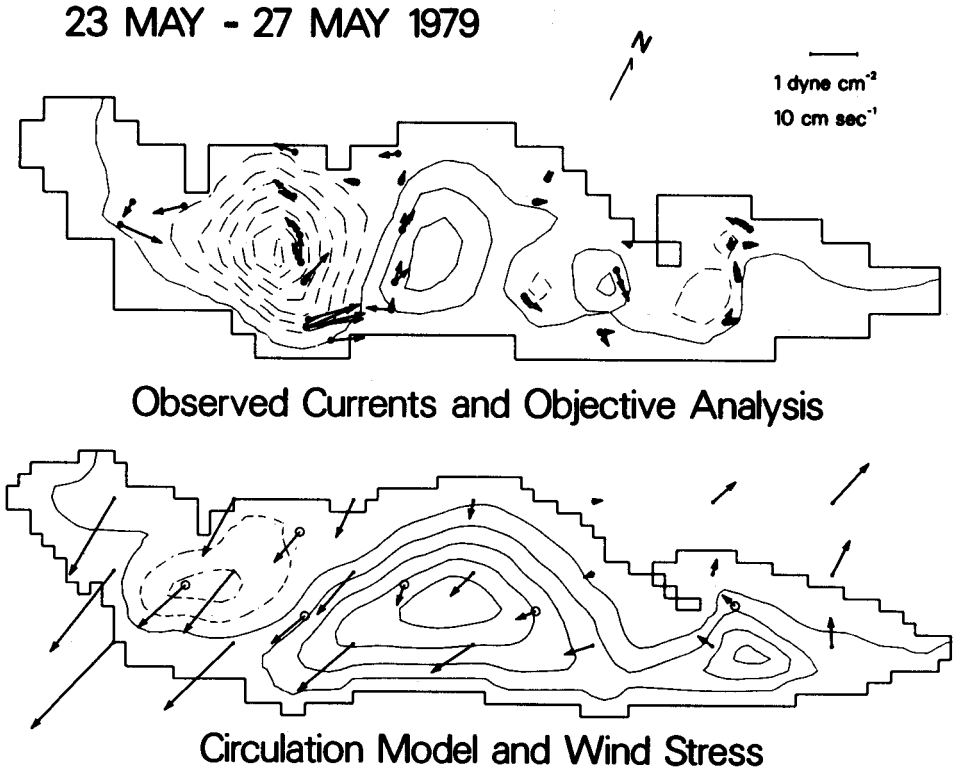

FIG. 3. Comparison of average stream functions from objective analysis and from numerical circulation model for the 23 - 27 May case. Also shown are average observed currents (top panel), average observed wind stress (lower panel, open circles), and average interpolated wind stress from numerical model run (lower panel). Negative values of stream function are indicated by dashed lines.

RESULTS AND DISCUSSION

Objective Analysis and Circulation Model

Maps were produced of the 5-day average stream function field from the objective analysis procedure and from the circulation model results for each case. Three representative comparisons are presented in Figures 3–5. Saylor and Miller (1987) pointed out three predominant patterns in Lake Erie's circulation and we tried to choose a sample of each.

Figure 3 shows the objectively analyzed and numerically modeled circulation patterns for the 23–27 May case. It also represents the most common pattern observed by Saylor and Miller (1987). The dominant wind direction during this period is north-northeast. Both the objectively analyzed and numerically modeled circulation patterns show a counterclockwise gyre in the western part of the lake and mainly clockwise circulation in the central part, although this pattern is disrupted in the objective analysis by two moorings in the central basin near the southern shore where eastward flow was observed. The clockwise gyre in the central basin is much stronger in the numerical model and the counterclockwise gyre is stronger in the objective analysis. In the eastern basin, the objective analysis shows a two-gyre pattern similar to Saylor and Miller (1987) while the numerical model produces strictly clockwise flow. As shown in Figure 2, this case also corresponds to the highest amount of kinetic energy observed in the lake during the experiment.

The objective analysis pattern for this case points out one of the shortcomings of using a purely objective scheme in analyzing currents from a sparse measurement array. In order to match the observed currents in the ridge area (Area 3 in Fig. 1) while still maintaining mass conservation, the objective analysis scheme has to produce

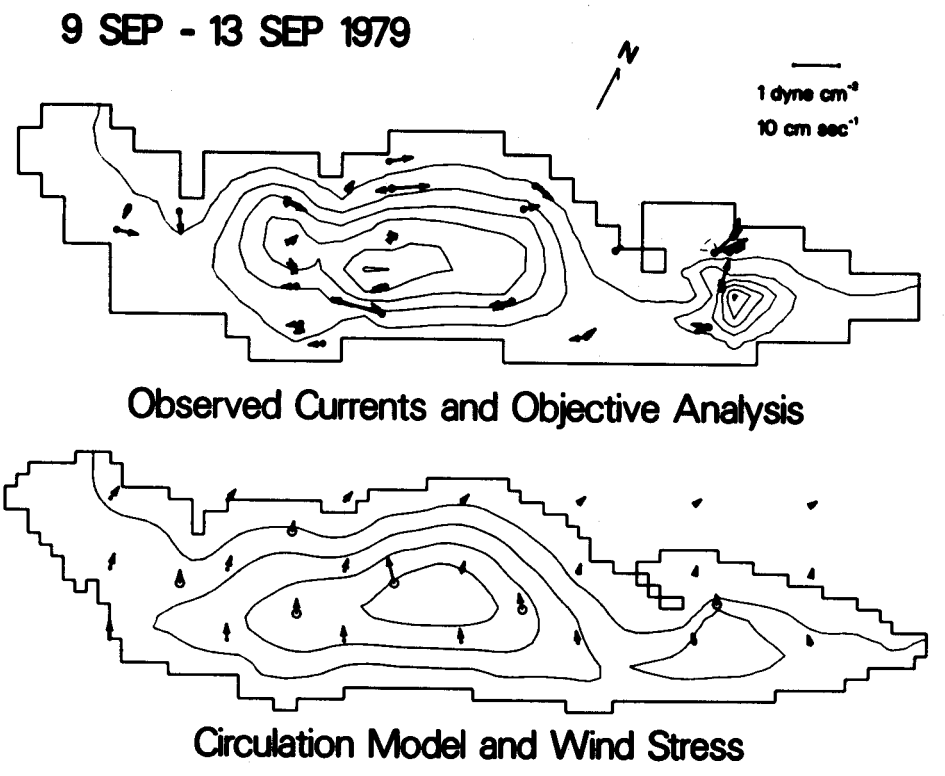

FIG. 4. Comparison of average stream functions from objective analysis and from numerical circulation model for the 9 - 13 September case. Also shown are average observed currents (top panel), average observed wind stress (lower panel, open circles), and average interpolated wind stress from numerical model run (lower panel). Negative values of stream function are indicated by dashed lines.

a complicated circulation pattern. In reality, the eastward flow at Moorings 20 and 23 may represent hypolimnetic return flow under the shallow thermocline that was destroyed by this storm. The total, vertically integrated flow could still be consistent with the westward direction shown by the numerical model.

One of the biggest shortcomings of the numerical model is that the components of the wind stress vector are approximated simply as linear functions of x and y (Eqs. 8 and 9). For the 23-27 May case, this results in the time averaged wind stress being southwestward in the ridge area and northward in the eastern basin. The mean spatially averaged wind stress over the eastern basin is therefore rather small so that the modeled circulation pattern in the eastern basin is dominated by the wind stress curl, producing a single clockwise gyre. If the wind stress were allowed to be more spatially uniform over the eastern basin while still maintaining the strong variation in the central basin, the mean circulation pattern in the eastern basin would be more like the objective analysis.

The 9-13 September case in Figure 4 shows strong clockwise circulation in both the objective analysis and in the circulation model results. When the mean longitudinal wind stress on Lake Erie is small, even a small curl in the wind stress field can overcome the two gyre pattern set up by a spatially uniform wind and cause a predominantly clockwise or counterclockwise pattern. This is mainly because the flat topography of the central basin diminishes strength of the classical two-gyre response to a uniform wind, allowing wind stress curl to have a greater influence on the resulting circulation pattern. This is probably why a single gyre circulation pattern is so frequently observed in the central basin.

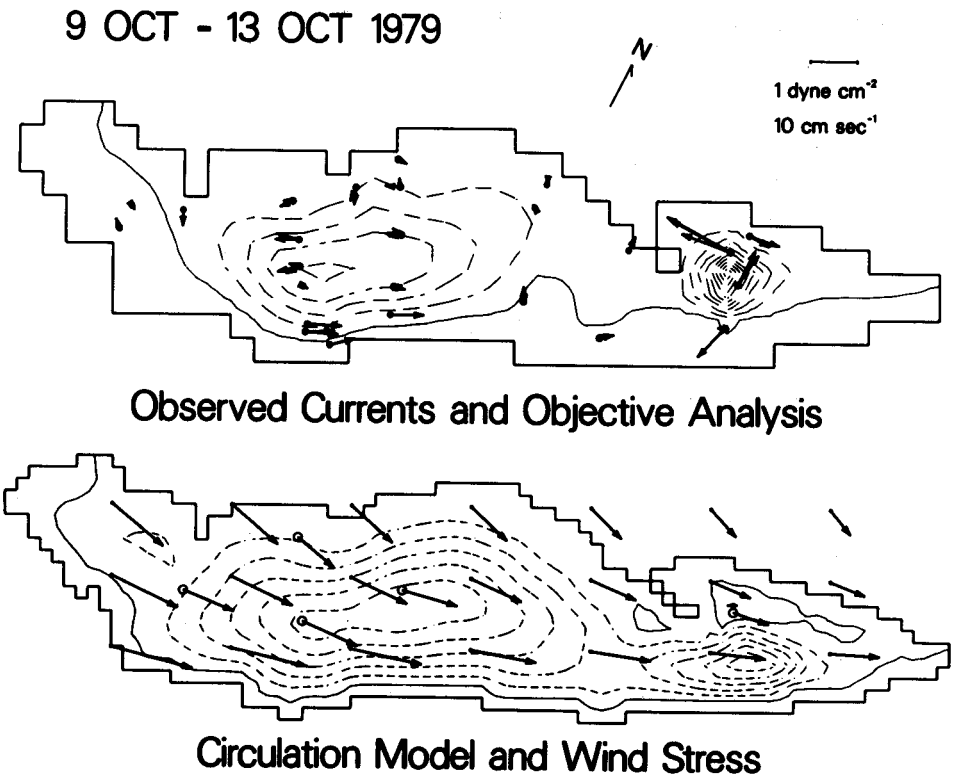

FIG. 5. Comparison of average stream functions from objective analysis and from numerical circulation model for the 9 - 13 October case. Also shown are average observed currents (top panel), average observed wind stress (lower panel, open circles), and average interpolated wind stress from numerical model run (lower panel). Negative values of stream function are indicated by dashed lines.

In Figure 5, the curl in the wind stress field is strong enough to overcome a relatively large mean longitudinal stress, this time resulting in a counterclockwise pattern. In the eastern basin, the model results still show a small clockwise cell in the northern part, but the strong measured currents at Mooring 27 seem to overwhelm the weak eastward flow at Mooring 28 in the objective analysis, resulting in a single counterclockwise gyre there. The counterclockwise circulation is much stronger in the model results than in the objective analysis.

Particle Trajectories

Figures 6–8 show the particle trajectories produced by the objectively analyzed and numerically modeled circulation fields for the same three cases for which average circulation patterns were presented in Figures 3–5. The large dots represent the 28 current meter moorings where the particles were released and the smaller dots show the particle locations after 1, 2, 3, 4, and 5 days.

In Figure 6 the objectively analyzed currents move some particles in the central basin as far as 20 km per day while the numerical model currents move them only half that far, reflecting the more intense counterclockwise gyre present in the objective analysis results in Figure 3. In the western basin, on the other hand, the numerical model currents are stronger than the objectively analyzed currents. The general direction of particle motion is similar in the objective analysis and the model results at most of the moorings with the most notable exceptions occurring in the southern part of the central basin. Particles from moorings 7 and 14 start out moving westward in both the objective analysis and the model, but reverse direction back to the east a day later in the model currents than in the objective analysis currents. This again is probably due to the fact that the counterclockwise gyre

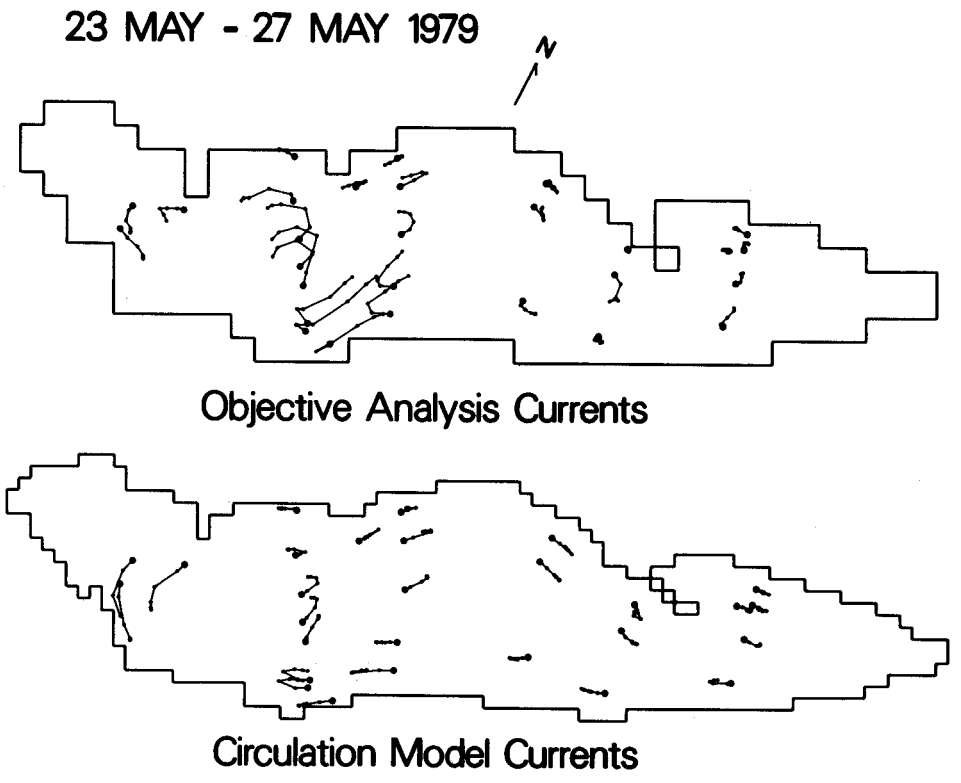

FIG. 6. Particle trajectories generated using objective analysis currents (upper panel) and numerical model currents (lower panel) for the 23 - 27 May case.

in the central basin is not as fully developed in the model results as in the objective analysis.

Figure 7 shows excellent agreement at nearly all locations in the central basin for the 9–13 September case, but poor agreement in the eastern basin. The numerical model results show persistent eastward currents along the north shore of the eastern basin while the observed currents turn back to the west after 2 or 3 days. This may be an indication of inadequate grid resolution in the eastern basin for the numerical calculation. During this case, particle displacements are as much as 5 km per day in the central basin and somewhat less in the eastern basin.

In the 9–13 October case in Figure 8, the currents from the numerical model are somewhat stronger than the objectively analyzed currents in the central basin, but directional agreement is quite good. The smooth trajectory of the particle released from mooring 17 near the southern shore of the central basin, even when it is near the corners of the numerical grid, is a reflection of the improved numerical scheme used to calculate the trajectories. Particle displacements are as high as 10 km per day in the numerical model results and somewhat less in the objective analysis.

A quantitative comparison of all the trajectories produced by the objective analysis currents and the numerical model currents is presented in Figure 9 and summarized in Table 1. The separation distance between particles which originated at the same location and the same time but were moved by either objective analysis currents or model currents are plotted against the distance traveled by the particle in the objective analysis currents separately for each case but grouped into the four geographic areas indicated in Figure 1. In Figure 9, the 1:1 diagonal line indicates a separation distance equal to the distance traveled. We consider this the dividing line between a skillful model prediction and one with no skill. It represents a prediction of no particle movement. The horizontal axis (separation distance = 0) represents perfect agreement between model results and observed currents. The

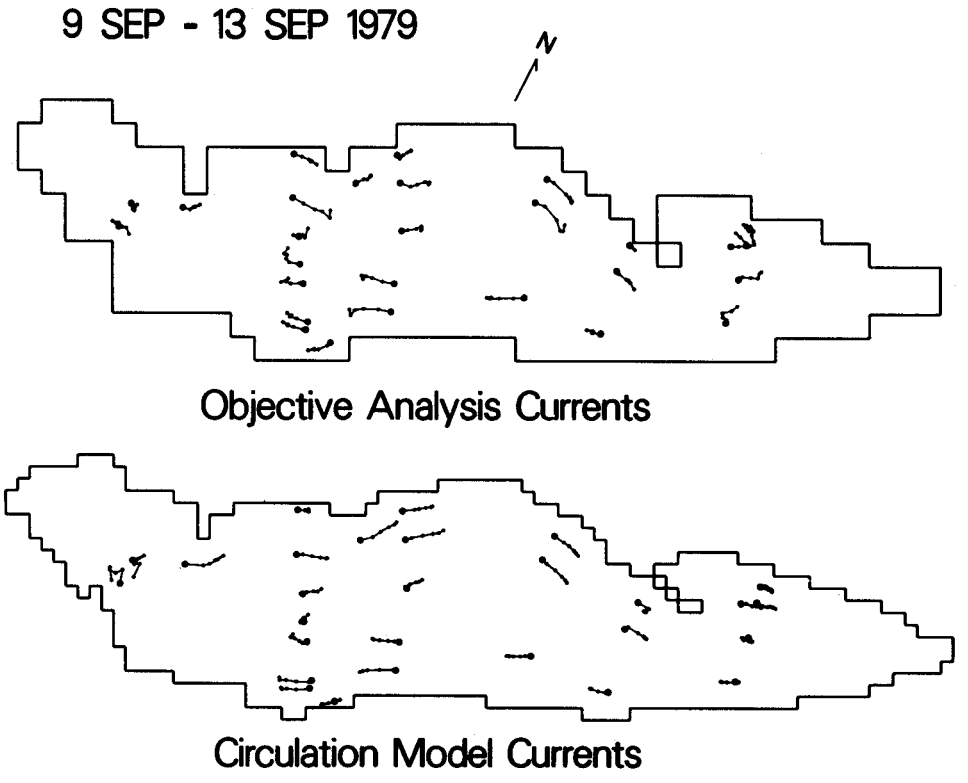

FIG. 7. Particle trajectories generated using objective analysis currents (upper panel) and numerical model currents (lower panel) for the 9 - 13 September case.

model shows least skill (virtually none) in Areas 1 and 4, some skill in Area 3 (particularly cases 3, 5, and 6), and the most skill in Area 2. Area 1 (the western basin) contained only three current meter moorings that were not well located to infer the circulation pattern in the western basin. In Area 4 (the eastern basin), the four moorings on a transect across the middle of the basin should provide at least an indication of the circulation pattern there. The differences between the observed and modeled circulation patterns may be due to the influence of baroclinic effects which are expected to be stronger in this deeper part of the lake or the fact that the 5-km grid resolution of the numerical model may not be adequate there.

Table 1 shows typical displacements from both objectively analyzed and numerically modeled circulation patterns on the order of 2.5–3 km per day. The numerical model produces much higher currents in the western basin (Area 1) than the objective analysis. This is probably due to the poor resolution of the observational array there. The other three areas show excellent agreement in mean path lengths. Mean separation distances are lower than mean path lengths in all areas except the eastern basin (Area 4). In Areas 2 and 3, the numerical model shows quite a bit of skill with mean separation distance to path length ratios of 0.57 and 0.76 respectively (using objective analysis path length). There is a tendency for the separation distance to grow more rapidly initially and then less rapidly after 2 or 3 days. This is reflected in the plots in Figure 9 as a tendency for the separation distance curves to flatten out with increasing distance traveled.

Finally, Figure 10 presents a composite map of the trajectories from all 12 cases. The purpose of this figure is to demonstrate the tendency of the objectively analyzed currents to show much more cross-isobath flow than the numerical model currents. This is probably due to the presence of meso-scale eddies whose influence survives the low-pass filter in the current meter records, or, perhaps, divergent flows not filtered out of the observed currents, although any energy at the fundamental barotropic seiche period of Lake Erie

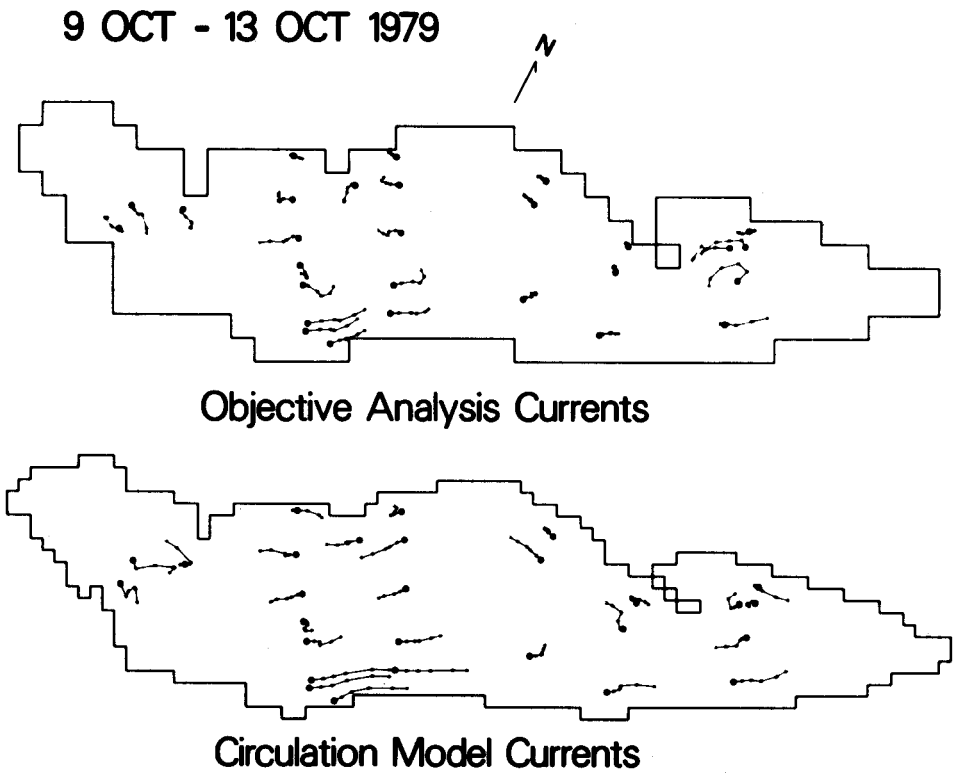

FIG. 8. Particle trajectories generated using objective analysis currents (upper panel) and numerical model currents (lower panel) for the 9 - 13 October case.

(about 14-h) should have been removed. The figure also shows the poor overall agreement between observed and modeled currents on the north and south shores of the eastern basin. The model results are almost always consistent with a two-gyre pattern in the eastern basin, with eastward flow near the north and south shores and westward return flow in the center of the basin. The observed currents are much more variable across the entire basin. As mentioned previously, this may be due to baroclinic effects, inadequate grid resolution in the numerical model, or poor resolution of the spatial variation in the wind field.

CONCLUSIONS

The results of an objective analysis technique for currents in a lake and the output of a numerical circulation model were compared for 12 5-day cases in Lake Erie by using Lagrangian tracer particles. The Lagrangian comparison technique has the advantage of integrating the circulation pattern as opposed to single point vector time series comparisons. We found that the circulation model showed considerable skill in predicting particle trajectories in areas where observational data were sufficiently dense for an accurate objective analysis. Results were not as good in areas with less dense coverage. Possible problems with the numerical model include inadequate grid resolution (particularly in the eastern basin), exclusion of baroclinic effects from the model, and oversimplification of the spatial variability of the wind stress field. The results of Bennett and Campbell (1987) show that the 5-km grid resolution used here might not be adequate in all parts of the lake, but this grid size was a computational limit in our calculations so we could not test smaller grid sizes. The importance of baroclinic effects on numerical circulation models over these time scales has yet to be adequately examined, although Schwab (1983) had very good results with a barotropic model in Lake Michigan, even during the stratified season. We are currently developing better wind interpolation schemes and hope to examine their effects on calculated circulation patterns in a further study.

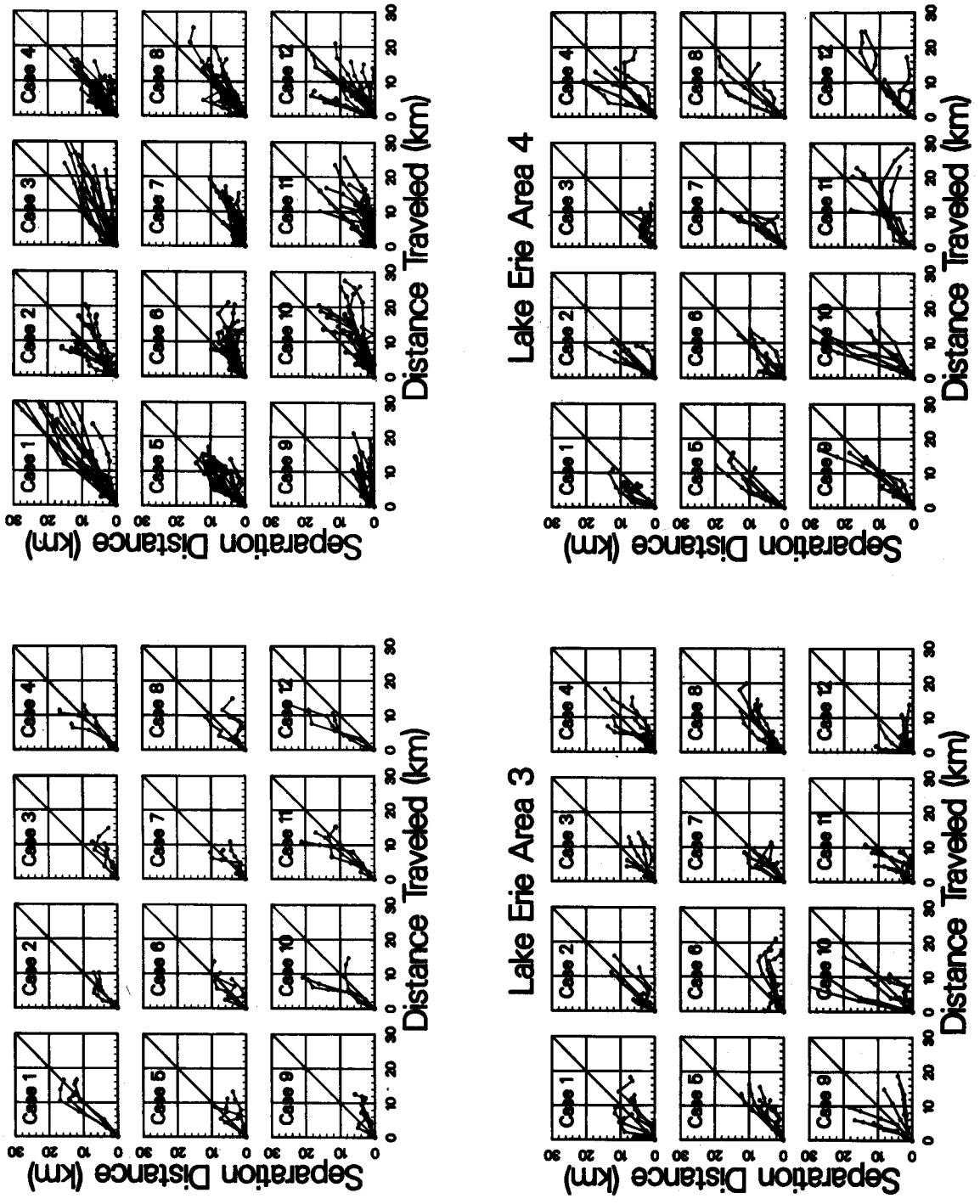

FIG. 9. Comparison of separation distance between particles in objective analysis current field and numerical model current field to distance traveled by particle in objective analysis current field. Comparisons are plotted for each case (see Fig. 2) and are grouped by area (see Fig. 1).

TABLE 1. Comparison of trajectories from objective analysis currents and from circulation model currents (distance in km).

Day:	1	2	3	4	5
Area 1					
Path Length					
Objective Analysis	2.16	4.95	7.29	9.37	11.25
Circulation Model	3.13	8.35	13.20	15.98	19.31
Separation Distance	2.50	5.11	7.50	9.05	9.94
Area 2					
Path Length					
Objective Analysis	2.45	5.42	9.06	12.25	14.90
Circulation Model	2.03	4.88	8.05	10.79	13.17
Separation Distance	2.00	3.89	5.48	7.39	8.49
Area 3					
Path Length					
Objective Analysis	1.75	4.08	6.12	8.16	10.27
Circulation Model	1.83	4.46	7.28	9.52	11.53
Separation Distance	1.78	3.60	5.30	6.92	7.79
Area 4					
Path Length					
Objective Analysis	2.25	4.79	7.45	9.80	12.20
Circulation Model	1.69	4.01	6.66	9.07	11.03
Separation Distance	3.31	6.19	8.01	9.98	11.76

One interesting result of the numerical model runs was that the bottom drag coefficient had to be adjusted upward in order to reproduce observed mean current speeds. In a similar study in Lake Michigan, Schwab (1983) found that the numerical model *under*estimated observed currents by a factor of two. In this study, observed currents were *over*estimated by the same factor before the bottom drag coefficient was adjusted.

The objective analysis techniques developed here was shown to be a useful tool for generating a lake-scale circulation pattern from an array of fixed current meters. The method faithfully reproduces observed currents at observation points and tends to predict zero current in areas removed from observation points. The main limitation of the technique is that it requires a sufficiently dense array to resolve the dominant scales of motion. Given an adequate observational array, the method is quite versatile.

REFERENCES

Bennett, J. R., and Campbell, J. E. 1987. Accuracy of a finite difference method for computing lake currents. *J. Comp. Phys.* 67:262-271.

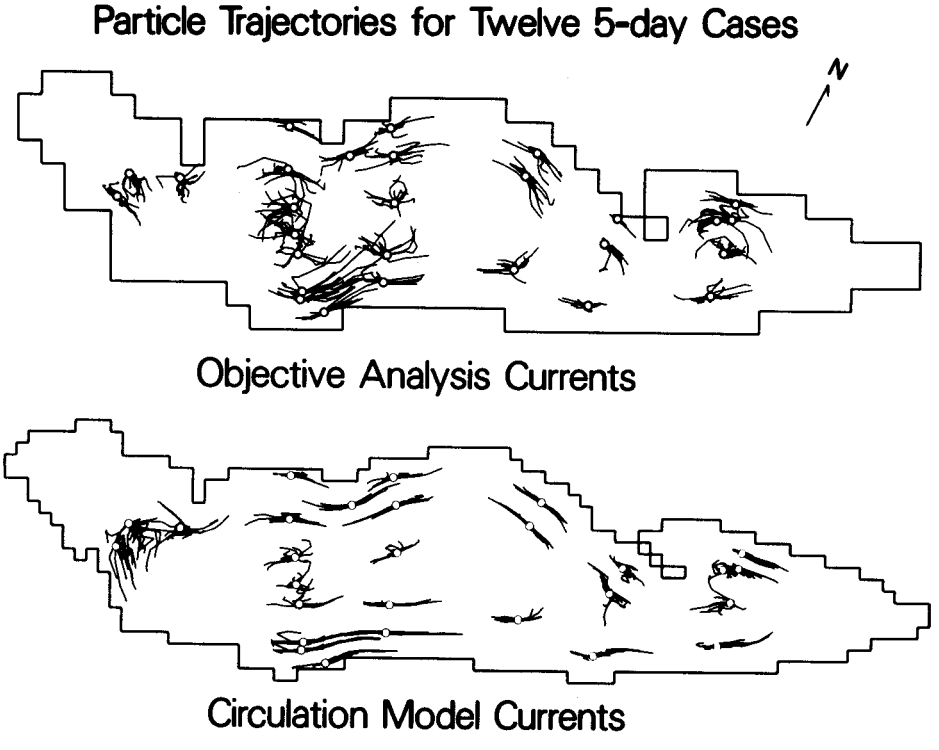

FIG. 10. Consolidated plot of trajectories for all 12 cases.

_____, and Clites, A. H. 1987. Accuracy of trajectory calculation in a finite difference circulation model. *J. Comp. Phys.* 68:272–282.

Businger, J. A., Wyngaard, J. C., Izumi, Y., and Bradley, E. F. 1971. Flux-profile measurements in the atmosphere surface layer. *J. Atmos. Sci.* 28:181–189.

Charnock, H. 1955. Wind stress on a water surface. *Quart. J. Roy. Meteor. Soc.* 81:639.

Freeland, H. J., and Gould, W. J. 1976. Objective analysis of mesoscale ocean features. *Deep-Sea Res.* 16 (Suppl.):58–71.

Galt, J. A. 1980. A finite-element solution procedure for the interpolation of current data in complex regions. *J. Phys. Oceanogr.* 10:1984–1997.

Lam, D. C. L. 1981. Temporal and spatial constraints in data estimation problems. *Appl. Math. Notes* 6:20–33.

Murthy, C. R., and Dunbar, D. S. 1981. Structure of the flow within the coastal boundary layer of the Great Lakes. *J. Phys. Oceanogr.* 11:1567–1577.

Rao, D. B., and Schwab, D. J. 1981. A method of objective analysis for currents in a lake with application to Lake Ontario. *J. Phys. Oceanogr.* 11:739–750.

Saunders, P. 1983. Benthic observations on the Madeira Abyssal Plain: currents and dispersion. *J. Phys. Oceanogr.* 13:1416–1429.

Saylor, J. H., and Miller, G. S. 1987. Studies of large-scale currents in Lake Erie, 1979–80. *J. Great Lakes Res.* 13:487–514.

Schwab, D. J. 1979. Simulation and forecasting of Lake Erie storm surges. *Mon. Wea. Rev.* 106:1476–1487.

_____ 1983. Numerical simulation of low-frequency current fluctuations in Lake Michigan. *J. Phys. Oceanogr.* 13:2213–2224.

_____, Bennett, J. R., and Jessup, A. T. 1981. *A two-dimensional lake circulation modeling system.* NOAA Tech. Memo. ERL GLERL-38, Great Lakes Env. Res. Lab., Ann Arbor, Michigan.

Simons, T. J. 1976. Continuous dynamical computations of water transports in Lake Erie for 1970. *J. Fish. Res. Board Can.* 33:371–384.

_____ 1980. Circulation models of lakes and inland seas. *Can. Bull. Fish. Aquatic Sci.* 203.

_____ 1985. Reliability of circulation models. *J. Phys. Oceanogr.* 15:1191–1204.